JPNT 8(2), 87-94 (2019)
https://doi.org/10.11003/JPNT.2019.8.2.87

JPNT Journal of Positioning, Navigation, and Timing

Performance Analysis of Long Baseline Relative Positioning using Dual-frequency GPS/BDS Measurements

Byung-Kyu Choi[1†], Ha Su Yoon[1], Sang Jeong Lee[2]

[1]Space Science Division, Korea Astronomy and Space Science Institute, Daejeon 34055, Korea
[2]Department of Electronics Engineering, Chungnam National University, Daejeon 34134, Korea

ABSTRACT

The Global Navigation Satellite System (GNSS) Real-Time Kinematic (RTK) positioning has been widely used in geodesy, surveying, and navigation fields. RTK can benefit enormously from the integration of multi-GNSS. In this study, we develop a GPS/BeiDou Navigation Satellite System (BDS) RTK integration algorithm for long baselines ranging from 128 km to 335 km in South Korea. The positioning performance with GPS/BDS RTK, GPS-only RTK, and BDS-only RTK is compared in terms of the positioning accuracy. An improvement of positioning accuracy over long baselines can be found with GPS/BDS RTK compared with that of GPS-only RTK and that of BDS-only RTK. The positioning accuracy of GPS/BDS RTK is better than 2 cm in the horizontal direction and better than 5 cm in the vertical direction. A lower Relative Dilution of Precision (RDOP) value with GPS/BDS integration can obtain a better positional precision for long baseline RTK positioning.

Keywords: GNSS, RTK, long baselines, integration

1. INTRODUCTION

The real-time kinematic (RTK) relative positioning and precise point positioning (PPP) are two of the typically used methods in positioning determination using global navigation satellite systems (GNSS). These methods have been widely used in geodesy, surveying, navigation, and earth science fields using GNSS (Zumberge et al. 1997, Kouba & Héroux 2001, Gao et al. 2005).

GNSS analysis centers started providing precise satellite orbits and satellite clock products. The positioning accuracy has improved for recent PPP users using these information. In the past, user's precise positioning was calculated using measurement data and products from only GPS and GLONASS in the existing PPP. More recently, however, user's position accuracy has improved significantly in the current PPP as precise satellite orbits and clock products of Galileo in the European Union, BeiDou in China, and Japanese Quasi-Zenith satellite system (QZSS) in addition to GPS and GLONASS were provided by GeoForschungsZentrum in Germany and Wuhan University in China. The problem is that PPP requires at least 20 min in the early converging stage to obtain the user's accurate position information. To overcome this problem, a number of studies have been conducted such as the use of multi-GNSS observation data (Cai & Gao 2013, Zhao et al. 2013, Cai et al. 2015), the use of improved upper atmospheric model (Hernández-Pajares et al. 2007, Elmas et al. 2011), and PPP Ambiguity Resolution (AR) (Ge et al. 2008, Geng et al. 2010). The initial convergence time was dramatically reduced to less than five min by applying the PPP AR among the above methods. However, some limitations in PPP still needed to be overcome such as initial convergence speed and real-time utilization.

The RTK does not need precise satellite orbits and clocks in contrast to PPP. On the other hand, the RTK requires

Received Feb 18, 2019 **Revised** Mar 10, 2019 **Accepted** Apr 15, 2019
†**Corresponding Author**
E-mail: bkchoi@kasi.re.kr
Tel: +42-865-3237 Fax: +82-42-861-5610

Byung-Kyu Choi https://orcid.org/0000-0003-2560-6714
Ha Su Yoon https://orcid.org/0000-0001-9917-5246
Sang Jeong Lee https://orcid.org/0000-0002-9400-5157

Copyright © The Institute of Positioning, Navigation, and Timing

correction information about state space representation from GNSS reference station network or observation data from specific GNSS reference station. GNSS reference station should have its own accurate position information. The performance of RTK is dependent on the baseline range between the reference station and user. Assuming that there is no rapid change in the ionosphere and troposphere in a short baseline within 20 km, the integer ambiguity number is easily determined thereby a positioning accuracy within a several cm distance can be obtained (Wielgosz et al. 2005). However, GNSS signals passing through the upper atmosphere change in a medium baseline from 20 km up to 100 km of the baseline distance so these elements are not removed even by a numerical differencing method. As a result, the degradation of probability that determines the integer ambiguity and a longer initial convergence time happen due to the residual error. These will eventually cause the reduction in positioning accuracy of users (Teunissen 1995). The upper atmosphere and reduction in the number of common satellites are more influential in a long baseline whose baseline distance is over 100 km than in a medium baseline. The users of GNSS dual-frequency receivers may improve the position accuracy by nearly removing the error due to the ionosphere, which is the largest error in the signal transmission. However, since users of GNSS single frequency receivers do not remove the ionospheric error directly, the error is separately estimated or models and global ionosphere maps products are additionally utilized to improve the location accuracy. However, the RTK performance of single frequency users in medium and long baselines is still poor compared to that of dual-frequency users.

China has developed a GNSS system called BeiDou (BDS) and aims to operate the system in full scale by 2020. The regional navigation satellite system (RNSS) has been already completed, which consists of five satellites in the geostationary earth orbit and five satellites in the inclined geosynchronous orbit. Since BeiDou RNSS is operated intensively in South East Asia, studies on precise positioning using GPS and BDS have been conducted (Chen et al. 2016, Paziewski & Sieradzki 2017).

In this study, we develop a relative positioning algorithm using GPS and BDS observation data and analyzes the positioning performance for the long baselines between a reference station and rovers. In addition, the data processing methods according to each baseline distance are divided into GPS-only, BDS-only, and integrated GPS+BDS and applied in order to compare the position accuracy. The effect of relative dilution of precision (RDOP) in the relative positioning determination is also considered.

Table 1. Processing strategy for long-baseline relative positioning.

Item	Models & Methods
GNSS observations	GPS, BDS
Frequencies	GPS L1 & L2, BDS B1 & B2
Baseline lengths	128, 216, 335 km
Sampling rate	30 s
Troposphere	GMF/GPT2
Ionosphere	Eliminated by IF linear combination
Tidal effect	IERS conventions 2010 & FES2004
PCO & PCV	IGS14.atx
Ambiguity	Float solution
Elevation cut-off angle	10 deg
Processing filter	Extended Kalman filter

2. DATA PROCESSING METHOD

Data processing methods, tropospheric delay error, and ionospheric delay error are some of the largest factors that influence the user's position accuracy in relative positioning. In particular, user's positioning errors increase as the baseline distance is longer between the reference station and user. This is directly related to the ionospheric delay error. That is, residuals due to double differencing (DD) become larger because paths where GNSS signals pass through the ionosphere become more different in the reference station and user as the baseline distance increases. More than 99% of the ionospheric error acted as a large error according to the baseline distance can be removed by the ionosphere-free (IF) linear combination of dual frequency as presented in Eqs. (1) and (2).

$$P_{IF} = \frac{f_1^2}{f_1^2 - f_2^2} P_1 - \frac{f_2^2}{f_1^2 - f_2^2} P_2 \tag{1}$$

$$\Phi_{IF} = \frac{f_1^2}{f_1^2 - f_2^2} \Phi_1 - \frac{f_2^2}{f_1^2 - f_2^2} \Phi_2 \tag{2}$$

Here, P_1 and P_2 are respective code observation values and Φ_1 and Φ_2 are carrier phase. f_1 and f_2 are frequencies of the two carrier phases. This study employs GPS L1 (1575.42 MHz) and L2 (1227.60 MHz) signals, and BDS's B1 (1561.098 MHz) and B2 (1207.17 MHz) signals.

Table 1 presents the data processing strategy used in the relative positioning determination. For the baseline length (BL) between the reference station and user, three BLs are selected: 128 km, 216 km, and 335 km. Parameters such as location and the integer ambiguity are estimated in every 30 sec using the Extended Kalman Filter. This study also uses Global Mapping Function (GMF) and Global Pressure and Temperature (GPT) 2 models to estimate the tropospheric delay error.

The tidal effect due to the Earth and the pole was compensated by using a model provided by the International earth rotation service (IERS) conventions 2010, and the effect of ocean tide was compensated by using the Finite Element

https://doi.org/10.11003/JPNT.2019.8.2.87

Solution (FES) 2004 model. For the phase center offset (PCO) and phase center variation (PCV) of the GNSS satellites and receiver's antenna, the IGS14.atx files that contained antenna information were used. The antenna information in the IGS14.atx files was updated in early 2017 replacing the existing IGS08.atx based on the International Terrestrial Reference Frame 2014. Although the tidal effect slightly varies according to regions, it may reach up to 30 cm in the altitude direction in the Korean Peninsula. In addition, the value of PCO differs depending on the receiver type, and the PCV shows a several cm difference before and after its application.

To determine the user position precisely through relative positioning, a reference satellite should be selected in a satellite constellation received in the observation time. In this study, a satellite that elevation angle is the highest was selected as a reference satellite and the reference satellite changes according to the observation time. The relative positioning requires reference station (RS) mandatorily in contrast to the PPP. The receiver and satellite clock error, which acts as the largest error in the observation data, is removed by performing double differencing using the selected reference station and reference satellite. As mentioned above, GNSS signals that passes through the upper layer atmosphere differs as the BL between the reference station and user is far, and most of the ionospheric delay error can be removed by the IF linear combination in the dual-frequency receivers. Thus, tropospheric delay error, different tidal effect between the reference station and user, and estimation of ambiguities are important factors that should be considered in long baseline relative positioning. Eqs. (3) and (4) present the double-differenced measurement equation.

$$P_{ru}^{kj} = \rho_{ru}^{kj} + T_{ru}^{kj} + \Delta dist_{ru} + \varepsilon_P \tag{3}$$

$$\Phi_{ru}^{kj} = \rho_{ru}^{kj} + T_{ru}^{kj} + \Delta dist_{ru} + N_{ru}^{kj} + \varepsilon_\Phi \tag{4}$$

Here, P_{ru}^{kj} refers to a double-differenced pseudorange value, Φ_{ru}^{kj} refers to a double-differenced carrier phase value, ρ_{ru}^{kj} refers to a double differenced value of geometry range between the satellite and receiver, T_{ru}^{kj} refers to a double-differenced tropospheric delay error value, N_{ru}^{kj} refers to a double differenced float ambiguities, $\Delta dist_{ru}$ refers to a difference in tidal effects between the reference station and user, and ε_P and ε_Φ refer to the pseudorange and carrier measurement noise, respectively. In addition, r and u refer to the reference station and user, respectively, k refers to the GPS reference satellite or BDS reference satellite, and j refers to GPS and BDS satellites. The initial dynamic variances and measurement noise for user location, tropospheric delay error, and float ambiguities were set as follows: 60.0^2, 0.3^2, 100.0^2 and 10.0^2, 0.001^2, 0.0, respectively

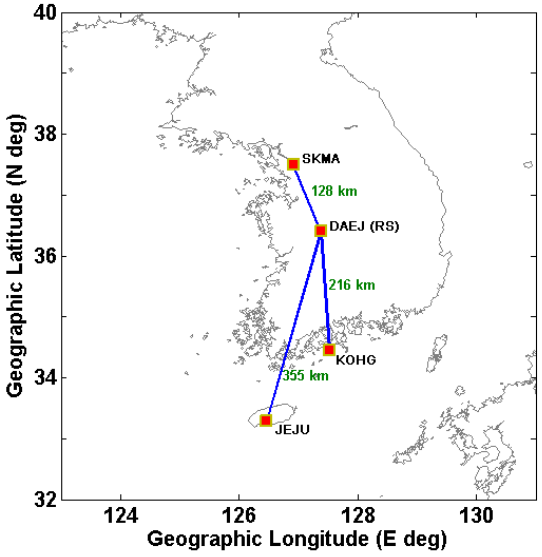

Fig. 1. Test configuration for GPS/BDS long-baseline relative positioning.

Table 2. GNSS receiver types on RS and rover stations.

Baseline	Reference receiver	Rover receiver	BL (km)
DAEJ – SKMA	Trimble NetR9	Trimble NetR9	128
DAEJ - KOHG		Trimble NetR9	216
DAEJ - JEJU		Trimble NetR9	335

3. RESULTS AND ANALYSIS

A total of three relative baselines were selected based on the DAEJ GNSS RS for the long baseline relative positioning experiment using GPS and BDS system. The baselines consist of DAEJ-SKMA, DAEJ-KOHG, and DAEJ-JEJU, respectively. The BLs were approximately 128 km, 216 km, and 355 km from the RS. The configuration of the baselines for the long baseline relative positioning is shown in Fig. 1 in detail. Table 2 presents the RS and GNSS receiver types of the users. DAEJ as the RS employs Trimble NetR9 receiver, and SKMA, KOHG, and JEJU, which were consisted of users, employ the same type of receivers used in the RS. The Trimble NetR9 used in the experiment can receive navigation signals from GPS, GLONASS, Galileo, BeiDou, and QZSS.

Fig. 2 shows the ground trajectory of GPS and BDS navigation satellites observed on January 1, 2019. The green-dotted line indicates GPS satellite's ground trajectory, and the red-dotted line indicates the BDS satellite's ground trajectory. There are 31 GPS satellites and 13 BDS satellites being operated, respectively. Note that a total of 10 satellites including five satellites in the geostationary orbit and five

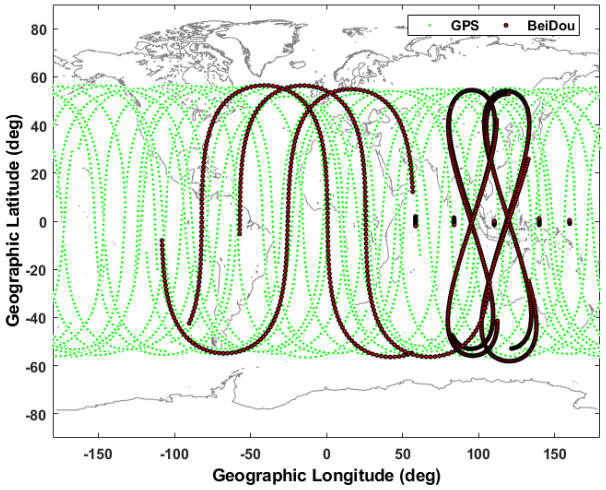

Fig. 2. Ground tracks of GPS satellites and BeiDou satellites on 1 January 2019.

satellites in the inclined geosynchronous orbit are operated for the BDS as the regional navigation system at the observation period on January 1, 2019. This characteristic of the BDS contributes to the improvement of user's position accuracy in a specific region (Gao et al. 2017).

3.1 Positioning Accuracy Analysis

Fig. 3 shows the position error in the navigation coordinate according to three different BLs in a time series. Data processing of GPS-only, BDS-only, and integrated GPS+BDS was performed respectively using the Multi-GNSS Analysis Software developed by the Korea Astronomy and Space Science Institute to compare and analyze the position error of relative positioning. In addition, the results calculated by high-precision GNSS software Bernese 5.2 developed by the University of Bern in Switzerland were assumed as the true value for high accuracy position of users in the comparative analysis of position error. Fig. 3a shows the calculation of position error in every 30 secs using the observation data of DAEJ and SKMA whose BL is 128 km. The red-dotted line and blue-dotted line indicate GPS-only and BDS-only, respectively, and the green solid line indicates the integrated GPS+BDS data processing result. As shown in the time series by position component in Fig. 3a, the location accuracy of GPS-only was superior compared to BDS-only. The figure shows that the position accuracy is significantly degraded particularly in the up direction in the case of BDS-only. The integrated GPS+BDS showed a slight improvement on initial convergence speed and position accuracy compared to those of GPS-only.

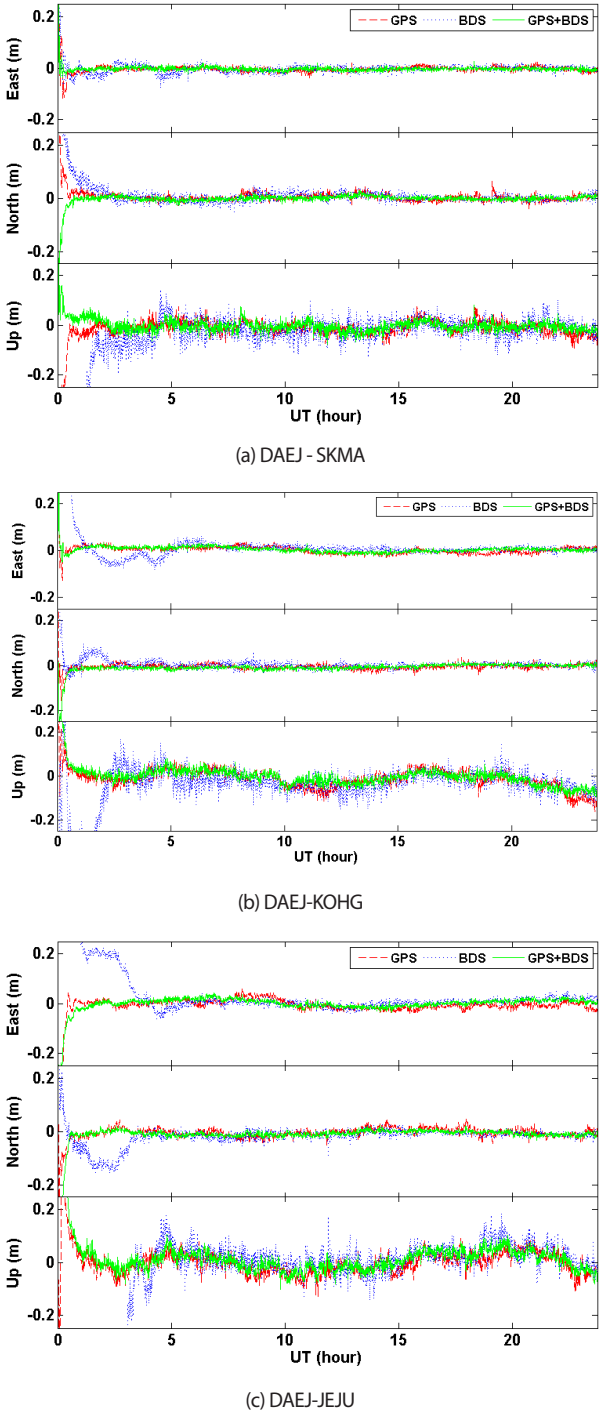

Fig. 3. Ground tracks of GPS satellites and BeiDou satellites on 1 January 2019.

Fig. 3b shows 216 km of BL, which is relatively longer than the previous BL. The position accuracy of BDS-only displayed with blue-dotted line was significantly reduced similar to the result in Fig. 3a. In addition to the reduction of position accuracy, the initial convergence speed was also slowed. Furthermore, the position precision of the up-direction

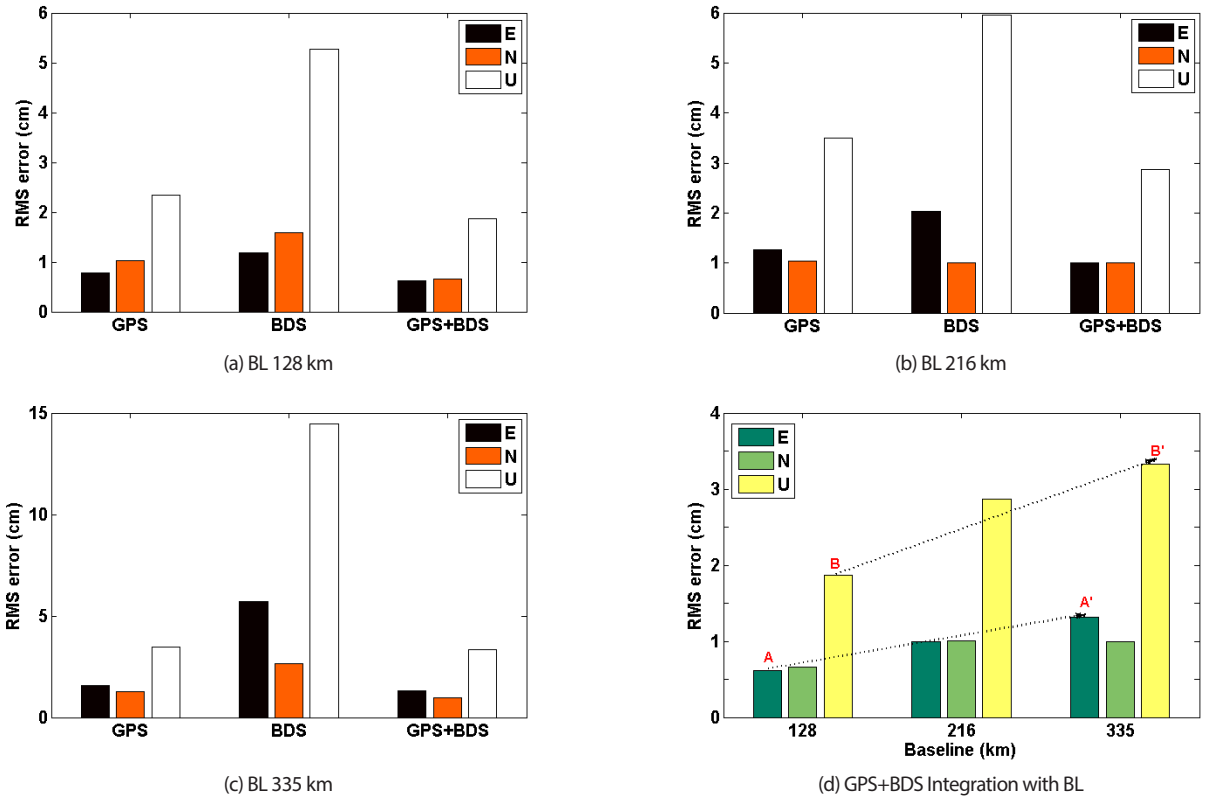

Fig. 4. Position RMS errors for GPS-only, BDS-only and GPS/BDS integration with BL: (a) 128 km, (b) 216 km, (c) 335 km and (d) GPS+BDS Integration with BL.

component for BDS-only was much degraded compared to that of BL-128 km. The integrated GPS+BDS result was very similar to that of GPS-only. Fig. 3c shows the data processing results between the regions in which BL is the longest. It shows similar results with those of the two relative baselines mentioned above. The position accuracy by the integrated GPS+BDS was nearly the same as that of GPS-only. Moreover, the position accuracy by BDS-only was degraded considerably compared to those of GPS-only and integrated GPS+BDS data processing results. In particular, the position error in the up direction component by BDS-only increased further. The data processing results on three BLs exhibited that the position errors of all GPS-only, BDS-only, and integrated GPS+BDS increased as the BL became longer. Note that the position error in the up direction component increased relatively more in BDS-only than in GPS-only as the BL became longer.

Fig. 4 shows the root mean square (RMS) value of position error according to each of the BLs by component. The RMS by component was calculated by setting the 95% confidence interval (2σ). Fig. 4a shows the position error at a region where the BL is 128 km. The results of GPS-only showed that both of the RMS errors in the east-west and south-north directions were less than 1 cm, and the position error in the up direction was approximately 2.3 cm. On the other hand, the results of BDS-only showed that the RMS error in the up direction was 5.2 cm, which revealed that the position accuracy was degraded more than twice compared to that of GPS-only. The results of integrated GPS+BDS showed that the positioning accuracy relatively improved more than those of GPS-only and BDS-only, particularly in the up direction. Fig. 4b and 4c show the position errors at 216 km and 335 km BLs, respectively. Compared to the result of Fig. 4a whose BL was 128 km, the position errors increased in all directions overall. In particular, the position error by BDS-only increased relatively more at 335 km BL. The position error increased approximately three times more in the east-west and up directions compared to that of BDS-only at 128 km BL. Based on the above results, the performance of long BL relative positioning using BDS was characterized by a significant degradation as the BL increased in a relative sense.

Fig. 4d shows the integrated GPS+BDS positioning results according to BLs. Interestingly, as the BL increased, a width ($B \rightarrow B'$) of increasing position error in the up direction was relatively larger than the width ($A \rightarrow A'$) of increasing in the east-west and south-north directions. This can be directly related to the increase of the position error in the up direction due to BDS.

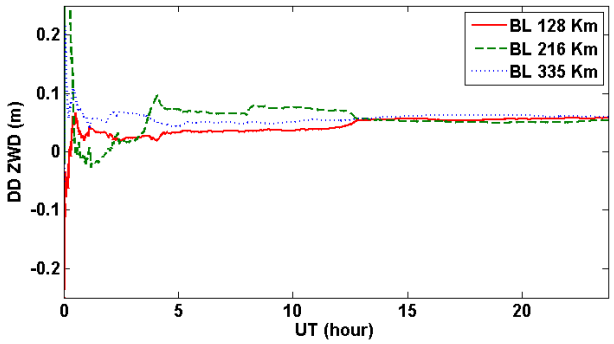

Fig. 5. Time series of estimated DD ZWD with BLs.

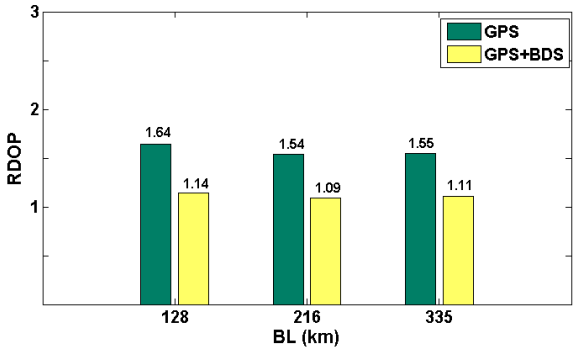

Fig. 6. Averaged RDOP vales in confidence level of 95 percent with BL.

Fig. 5 shows the estimated wet delay errors in the troposphere that are double differenced values with each of the BLs in a time series. The wet delay error in the troposphere is highly affected by the difference in atmospheric environment between the reference station and user. As shown in Fig. 5, the estimated values with each of the BLs change approximately within a range of 10 cm.

3.2 RDOP Analysis

DOP is an indicator that represents a level of geometry of GNSS satellite constellation. The precision probability becomes higher as the DOP value is smaller. Reversely, the precision probability is degraded as the DOP value increases. DOP can be expressed by the following indicators: horizontal DOP, vertical DOP, position DOP, time DOP, and geometric DOP. In this study, RDOP, which is an indicator that is related to user's position precision in relative positioning, was calculated by each of the BLs.

Eq. (5) presents the variance covariance matrix Q that should be calculated in advance to the computing of RDOP. Assuming that a size of the design matrix (H) in the linearized double differenced equation is $m \times 3$, Q becomes a square matrix whose size is 3×3. Once the variance covariance matrix is calculated, the RDOP can be calculated as presented in Eq. (6) using the variance values about position component among the diagonal terms in the matrix.

$$Q = (H^T H)^{-1} = \begin{bmatrix} \sigma_x^2 & \sigma_{xy} & \sigma_{xz} \\ \sigma_{xy} & \sigma_y^2 & \sigma_{yz} \\ \sigma_{xz} & \sigma_{yz} & \sigma_z^2 \end{bmatrix} \quad (5)$$

$$RDOP = \sqrt{\sigma_x^2 + \sigma_y^2 + \sigma_z^2} \quad (6)$$

Here, the RDOP value changes continuously as the position and GNSS satellite constellation changes over time. In addition, the change in the RDOP value is directly related to the number of visible satellites. Fig. 6 shows the RDOP value calculated using the observation data received at three BLs in a day on January 1, 2019. The RDOP value was calculated by each of GPS-only and integrated GPS+BDS, and daily averaged values were calculated within the 95% confidence interval.

The RDOPs by GPS-only were 1.64, 1.54, and 1.55 according to each BL, which were highly reliable values to obtain the position precision. In addition, very similar RDOPs were exhibited without a significant difference by BLs. The RDOP by the integrated GPS+BDS was relatively smaller than that of GPS-only. The smaller RDOP value indicated that more reliable position precision could be obtained. That is, the RDOP analysis suggests that the integration of GPS and BDS could improve position precision compared to that of GPS-only.

4. CONCLUSIONS

This study selected three BLs to comparatively analyze the positioning accuracy of relative positioning with regard to 100 km or longer BLs, and performed data processing using GPS-only, BDS-only, and integrated GPS/BDS, respectively. The data processing results revealed that position errors increased in all of GPS-only, BDS-only, and integrated GPS/BDS as the BL became longer. Note that the position accuracy of BDS-only was significantly degraded as the BL increased. In particular, the position error in the up direction component increased further.

The positioning accuracy of integrated GPS/BDS relatively improved more than those of GPS-only and BDS-only, in particular, in the up direction significantly. The comparison results of integrated GPS/BDS alone among three BLs showed that as the BL increased, an increasing magnitude of position error in the up direction was relatively larger than

that in the horizontal direction. This can be directly related to the increase in the position error of BDS-only in the up direction with increase in BL.

In addition, the RDOP, which is a reliable indicator in user's position determination, was calculated and analyzed. The RDOP according to BLs were very similar without a significant difference. The RDOP using only GPS-only was less than two in all BLs, which was highly reliable to obtain the position precision. In addition, the RDOP by the integrated GPS/BDS was smaller than that of GPS-only by 0.45 to 0.50 in all BLs in a relative sense. The smaller RDOP value indicated that more reliable position precision could be acquired. Conclusively, the integrated GPS/BDS could improve positioning accuracy and position precision compared to those of GPS-only and BDS-only.

Therefore, the integrated GPS/BDS in the long BL relative positioning can improve positioning accuracy and obtain more reliable position precision.

ACKNOWLEDGMENTS

This study was supported by the 2019 Primary Project of the Korea Astronomy and Space Science Institute (project: Space Environment Research).

AUTHOR CONTRIBUTIONS

Methodology, B.K.; software, B.K. and H.S.; formal analysis, B.K. and H.S.; investigation, B.K. and S.J.; visualization, B.K.

CONFLICTS OF INTEREST

The authors declare no conflict of interest.

REFERENCES

Cai, C. & Gao, Y. 2013, Modeling and assessment of combined GPS/ GLONASS precise point positioning, GPS Solut., 17, 223-236. https://doi.org/10.1007/s10291-012-0273-9

Cai, C., Gao, Y., Pan, L., & Zhu, J. 2015, Precise point positioning with quad-constellations: GPS, BeidDou, GLONASS and Galileo, ASR, 56, 133-143. https://doi.org/10.1016/j.asr.2015.04.001

Chen, J., Wang, J., Zhang, Y., Yang, S., Chen, Q., et al. 2016, Modeling and Assessment of GPS/BDS Combined Precise Point Positioning, Sensors, 1151. https://doi.org/10.3390/s16071151

Elmas, Z. G., Aquino, M., Marques, H. A., & Monico, J. F. G. 2011, Higher order ionospheric effects in GNSS positioning in the European region, Ann. Geophys., 29, 1383-1399. https://doi.org/10.5194/angeo-29-1383-2011

Gao, Y., Wojciechowski, A., & Chen, K. 2005, Airborne Kinematic Positioning Using Precise Point Positioning Methodology, Geomaica, 59, 29-36

Gao, Z., Ge, M., Shen, W., Li, Y., Chen, Q., et al. 2017, Evaluation on the impact of IMU grades on BDS + GPS PPP/INS tightly coupled integration, ASR, 60, 1283-1299. https://doi.org/10.1016/j.asr.2017.06.022

Ge, M., Gendt, G., Rothacher, M., Shi, C., & Liu, J. 2008, Resolution of GPS carrier-phase ambiguities in precise point positioning (PPP) with daily observations, J. Geod., 82, 389-399. https://doi.org/10.1007/s00190-007-0187-4

Geng, J., Meng, X., Dodson, A. H., Ge, M., & Teferle, F. N. 2010, Rapid re-convergences to ambiguity-fixed solutions in precise point positioning, J. Geod., 84, 705-714. https://doi.org/10.1007/s00190-010-0404-4

Hernández-Pajares, M., Juan, J. M., Sanz, J., & Orús, R. 2007, Second-order ionospheric term in GPS: implementation and impact on geodetic estimates, JGR, 112: B08417. https://doi.org/10.1029/2006JB004707

Kouba, J. & Héroux, P. 2001, Precise point positioning using IGS orbit and clock products, GPS Solut., 5, 12-28. https://doi.org/10.1007/PL00012883

Odijk, D. 2003, Ionospheric-Free Phase Combinations for Modernized GPS, Journal of Surveying Engineering, 129, 165-173. https://doi.org/10.1061/(ASCE)0733-9453(2003)129:4(165)

Paziewski, J. & Sieradzki, R. 2017, Integrated GPS+BDS instantaneous medium baseline RTK positioning: Signal analysis, methodology and performance assessment, ASR, 60, 2561-2573, https://doi.org/10.1016/j.asr.2017.04.016

Teunissen, P. J. G. 1995, The least-squares ambiguity decorrelation adjustment: A method for fast GPS integer ambiguity estimation, Journal of Geodesy, 70, 65-82. https://doi.org/10.1007/BF00863419

Wielgosz, P., Kashani, I., & Grejner-Brzezinska, D. 2005, Analysis of long-range network RTK during a severe ionospheric storm, J. Geod., 79, 524-531. https://doi.org/10.1007/s00190-005-0003-y

Zhao, Q., Guo, J., Li, M., Qu, L., Hu, Z., et al. 2013, Initial results of precise orbit and clock determination for COMPASS navigation satellite system, J. Geod., 87, 475-

486. https://doi.org/10.1007/s00190-013-0622-7
Zumberge, J. F., Heflin, M. B., Jefferson, D. C., Watkins, M. M., & Webb, F. H. 1997, Precise point positioning for the efficient and robust analysis of GPS data from large networks, J. Geophys. Res. Solid Earth, 102, 5005-5017. https://doi.org/10.1029/96JB03860

Byung-Kyu Choi received the Doctor's degree in Electronics in Chungnam National University in 2009. He has been working at the Korea Astronomy and Space Science Institute since 2004. His research interests include multi-GNSS PPP, PPP-RTK, and GNSS TEC estimation.

Ha Su Yoon received a Ph.D. degree in Department of Geoinformatics in University of Seoul in 2015. Since 2016, he has been with the Korea Astronomy and Space Science Institute. His current research interests include GNSS meteorology and ocean tide loading.

Sang Jeong Lee received the Doctor's degree in Control and Measurement in Seoul National University in 1987. His research interests include GNSS and Robust Control.